Mihailo Mrdak[1], Časlav Lačnjevac[2], Marko Rakin[3], Đorđe Janaćković[1], Darko Veljić[1], Darko Bajić[4]*

[1]University of Belgrade, Inovation Center - Faculty of Technology and Metallurgy, Belgrade, Serbia, [2]University of Belgrade, Faculty of Agriculture, Belgrade, Serbia,[3]University of Belgrade, Faculty of Technology and Metallurgy, Belgrade, Serbia, [4]University of Montenegro, Faculty of Mechanical Engineering, Montenegro

Scientific paper
ISSN 0351-9465, E-ISSN 2466-2585
UDC:666.3.019:620.197.6:621.793.74
https://doi.org/10.5937/zasmat2104262M

Zastita Materijala 62 (4)
262 - 268 (2021)

Characterisation of biocompatible layers of $ZrO_2 8\%Y_2O$ used in combination with other ceramics to modify the surface of implants

ABSTRACT

The aim of this study was to deposit multi-functional $ZrO_2 8\%Y_2O_3$ coating layers using the plasma spray technology and then to characterise such layers. In combination with other biomedical ceramics, this coating is intended for the application in implant surface modification. The examination was focused on the mechanical properties and microstructure layers . Using the atmospheric plasma spraying, duplex $ZrO_2 8\%Y_2O_3$/Ni22Cr10Al1Y coating system was deposited on the X15Cr13 stainless steel, with two different thicknesses of the bond and ceramic coatings. The microstructure was analysed using an optical microscope, including the assessment of the content of micropores. The morphology of powder particles and ceramic coating surfaces were examined on a scanning electron microscope (SEM). The quality of the $ZrO_2 8\%Y_2O_3$ layers makes them suitable for the application and combination with other materials to create a system of biomedical or multifunctional coatings.

Keywords: *Atmospheric plasma spray, $ZrO_2 8\%Y_2O_3$, Ni22Cr10Al1Y, microstructure, interface, microhardness, bond strength.*

1. INTRODUCTION

ZrO_2-Y_2O_3 ceramic has the highest level of toughness, strength and the best physical characteristics with regard to other inorganic ceramics. Today, due to these properties and its biocompatibility, it is used for implant surfaces as a biomaterial in combination with other materials. Hydroxyapatite (HA) organic ceramic, due to its low ductility, is not suitable as a standalone material for implant manufacturing. In order to improve its mechanical properties and osteoconductivity, HA ceramic is enhanced with a solid solution of the ZrO_2-8%Y_2O_3 oxides. Research results have shown that by adding $ZrO_2Y_2O_3$(YSZ) to hydroxyapatite, from 40 wt% to 60 wt%, its.decomposition is significantly decreased during the powder deposition using plasma spray. Higher content of Zirconium Oxide $ZrO_2Y_2O_3$(YSZ) increases the content of crystal HA and decreases the content of amorphous phases within the coating [1,2]. The atmospheric plasma spray (APS) and vacuum plasma spray (VPS) are the most convenient and cost-effective ways of depositing a large number of coatings, especially the coatings with different numbers of layer combinations made of different materials deposited on the metal surface of implants. Quick progress in terms of the development of new generations of implants for biomedical purposes has been enabled by using the plasma spray process and bioinert powdered metals and ceramics, both at the micro and nanolevels [3-5].

These possibilities of the plasma spray process significantly increase the resistance of an implant surface in terms of wear and tear, contact load, flexural strength, toughness and resistance to corrosion due to the impact of bodily fluids. These processes are characterised by the application of a wide range of bioinert metal and inorganic ceramic powders which are combined with organic ceramic. Zirconium dioxide $ZrO_2Y_2O_3$ is used as a bioinert ceramic in combination with hydroxyapatite, bioglass and calcium phosphate, due to its good

*Corresponding author: Mihailo Mrdak
e-mail: drmrdakmihailo@gmail.com
Paper received: 28. 06. 2021.
Paper accepted: 24. 07. 2021.
Paper is available on the website: www.idk.org.rs/journal

toughness, density and surface inertness [6,7]. Necessary theoretical knowledge, as well as practical experience, represent the foundation for the reliable engineering of quality coating, selection of powder and the type of the plasma spray process, definition of plasma spray parameters and completion of deposition with the aim of achieving the optimum coating quality. Christel et al. were the first to present the use of ZrO_2 for the production of the femoral heads for hip replacements, which is its major application in medicine today [8]. The most studied stabilisers for ZrO_2 are CaO, MgO, Y_2O_3 and CeO_2 [9-12], however, only $ZrO_28\%Y_2O_3$ meets the ISO standard for surgical application [13]. Testing the biocompatibility of ceramic powders such as $ZrO_28\%Y_2O_3$ showed that they do not cause cytotoxicity in living cells [14,15]. Today, ZrO_2 layers stabilised by Y_2O_3 are widely used in manufacturing hip joint replacements as well as in protecting the hip implant surface together with bioreactive layers of organic ceramic (HA). [16]. Additionally, due to good mechanical characteristics, primarily toughness and high stability, ZrO_2 ceramic is used as a dental implant [17]. Additionally, due to good mechanical characteristics, primarily toughness and high stability, ZrO_2 ceramic is used as a dental implant [18]. Since ZrO_2-Y_2O_3 ceramic turned out to be the most dominant inorganic ceramic in the implant manufacturing process, this created a need for the deposition of $ZrO_28\%Y_2O_3$ layers using plasma spray in order to analyse mechanical and structural characteristics of the ceramic.

By analysing the paper written by Marcelli at all [18], who used NiAlMo bond coating, we came to the idea to use Ni22Cr10Al1Y coating as a bonding layer. A typical microstructure of the plasma sprayed $ZrO_28\%Y_2O_3$ oxide is lamellar with horizontal and transverse cracks, unmolten particles and micropores. These defects in the microstructure are formed during the deposition of particles, which coincides with their velocity towards the substrate, collision speed with the substrate and the cooling rate. Deposited particles exhibit high residual stresses, arising from the difference between the thermal shrinkage of ZrO_2 in comparison with the substrate and extremely high cooling rate ~ 10^6 °C/s. There are two mechanisms of oxygen transfer through this coating: ionic diffusion of oxygen from ZrO_2 crystal structure and penetration of oxygen as a gas through micropores and microcracks [19]. The thickness of the oxide layer of the bond coating may be increased during the oxidation; this produces stresses on the bond-ceramic interface. These stresses cause cracking at the joint of the bond coating and ceramic YSZ (Yttria-stabilized Zirconia) layer [19]. Transverse and longitudinal cracks are formed on the surface or near the upper layer/interface of the bond and ceramic layer due to the thermal stresses that will cause cracking of the ceramic layer (partially or completely with flaking from the substrate). Generally, coating fractures represent a rather important topic, due to their inhomogeneity. Different approaches have been applied in the literature for the assessment of failure resistance of heterogeneous structures [20-23]. More details on the mechanical behaviour of coatings and biomaterial interfaces, including damage, fracture and corrosion resistance, can be found in [24-27].

The aim of this study was to characterise $ZrO_28\%Y_2O_3$ layers deposited by the APS process and produce the coatings with adequate quality for different applications, but primarily for surface modification of alloys for the fabrication of implants. In order to successfully use $ZrO_28\%Y_2O_3$ coating in combination with other ceramics, to create a system of biomedical coatings, it is necessary to deposit the layers without defects. For that cause, an analysis of the mechanical characteristics and structure of the layers was performed to assess the quality of the coating.The ceramic layers do not contain coarse cracks and pores, which confirmed that the layers were deposited within optimal deposition parameters.

2. EXSPERIMENTAL PART

2.1. Materials and experimental details of plasma spray coatings deposition

The Č.4171 (X15Cr13 - EN10027) stainless steel Železarna Ravne, Slovenia, was the substrate onto which the coating layers were deposited. AMDRY 9624 and Metco 204NS (Sulzer Metco) powders were used for the fabrication of a two-layer coating. AMDRY 9624 is Ni22Cr10Al1Y alloy based on Ni with 20 wt% Cr, 10 wt% Al and 1 wt% Y with the granulation range of 11 - 37 µm [28]. Figure 1 shows the secondary electron image (SEM) of this powder; the particles are spherical. Ceramic powder Metco 204NS is ZrO_2 stabilised with $8wt\%Y_2O_3$ which is produced by agglomeration and HOSP (Hollow Oxide Spherical Powder) technique. Granulation is in the range of 11-125 µm, the melting point is at 2800°C and thermal conductivity is 0.8-1.3 W/Mk [29]. Figure 2 (SEM image) reveals a spherical particle shape. The mechanical properties of the coating system were tested according to the standard PN 582005 [30]. The steel bases onto which the coatings were sprayed for microhardness and microstructure examination were 70x20x1.5 mm in size.

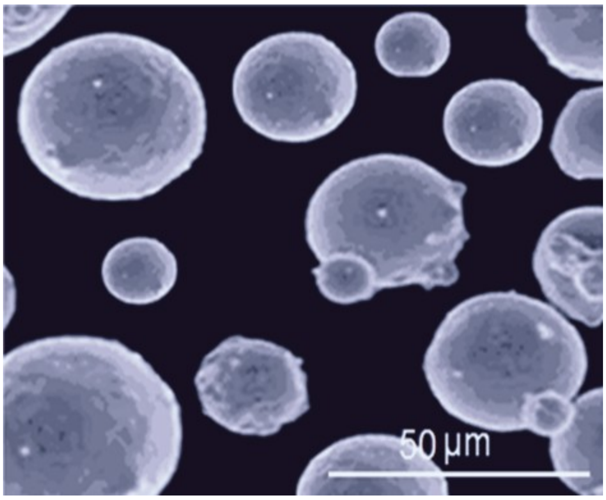

Figure 1. (SEM) Scanning electron micrograph of the Ni22Cr10Al1Y powder particles

Slika 1. (SEM) Skening elektronska mikrofotografija čestica praha Ni22Cr10Al1Y

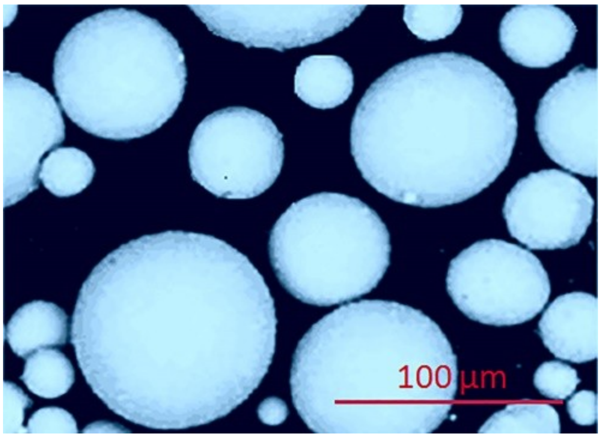

Figure 2. (SEM) Scanning electron micrograph of the $ZrO_2\ 8Y_2O_3$ powder particles

Slika 2. (SEM) Skening elektronska mikrofotografija čestica praha $ZrO_2\ 8Y_2O_3$

The size used for bond strength testing–adhesionwas Ø25x50mm. Measuring of microhardness ($HV_{0.3}$) was performed in the direction along the lamellae. Five readings of microhardness values of the layers were collected, in the middle and at the ends of the samples; two extreme values were discarded. Of the three remaining values, minimum and maximum are shown. Bond strength testing (adhesion) was conducted with a tension rate of 1 cm/min. The test groups consisted of five specimens (again, two extreme values were discarded). Of the three remaining values, the average bond strength is shown. The morphology of the powder particles was examined on SEM. Characterisation of the surface of the ceramic coating in the middle and 2 mm from the edge of the sample was also done on SE. The microstructure of the layers was examined under an optical microscope (OM). Analysis of the content of micropores in the coating was performed by examining 5 micrographs at 200X magnification. This paper presents the average value of the content of micropores. The deposition of the powders was done with the atmospheric plasma spray (APS) [31] system of the Plasmadyne Company and the SG-100 plasma gun, which consisted of a type K 1083A-129 cathode, type A 1083-165 anode and a type GI 1083A-113 gas injector. Argon was used as the arc gas, in combination with He and the power supply of up to 40kW. The plasma spray powder deposition parameters are shown in Table 1. Primary cooling of the molten powder particles in the process of deposition was carried out with dry compressed air, through two nozzles on the plasma gun. Before the powder deposition process, the substrate surfaces were roughened with white corundum particles, 0.7 - 1.5 mm in size. The powder was deposited on the substrate, preheated to 160-180 °C. Two groups of samples were made, with different thicknesses of bond coating/ceramic coating: (0.1-0.11mm/0.4-0.42 mm) and (0.2-0.25 mm/0.25-0.28 mm).

Table 1. Powder deposition parameters

Tabela 1. Parametri depozicije praha

Deposition parameters	AMDRY 9624	Metco 204NS
Plasma current, *I* (A)	800	900
Plasma voltage, *U* (V)	42	43
Primary plasma gas flow rate, Ar (l/min)	47	47
Secondary plasma gas flow rate, He (l/min)	22	32
Carrier gas flow rate, Ar (l/min)	9	6
Powder feed rate, (g/min)	35	45
Stand-off distance, (mm)	120	90

3. RESULTS AND DISCUSSION

3.1. Results of coatings testing

Microhardness values of the coatings system are shown in Figure 3. Ni22Cr10Al1Y alloy bond coating had consistent values in the range of 386-414 $HV_{0.3}$. Distribution of microhardness indicates that the layers were deposited uniformly throughout the coating cross-section with a small portion of micropores, confirmed by the analysis of the micrographs. The microhardness of the $ZrO_2 8\% Y_2O_3$ ceramic coating was 710 - 768$HV_{0.3}$. Due to the weaker inter-lamellar contact between the deposited particles, the ceramic coating had a wider microhardness range. The ceramic particles had less pronounced plastic deformation compared to particles of the metal coating in terms of the collision with the previously deposited layer. Therefore, the ceramic layers had a higher content of micropores, also confirmed by the analysis of the micrographs.

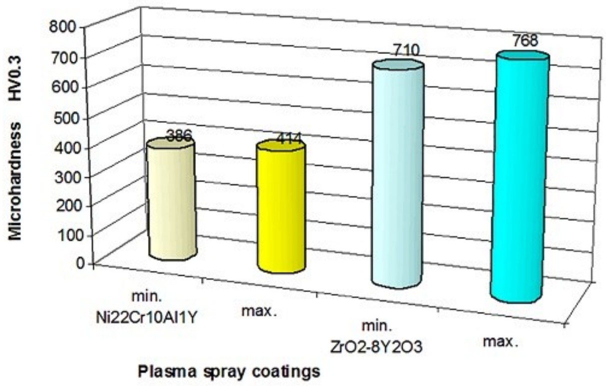

Figure 3. Results microhardness of the coating Ni22Cr10Al1Y and $ZrO_2 8\% Y_2O_3$

Slika 3. Rezultati mikrotvrdoće prevlaka Ni22Cr10Al1Y i $ZrO_2 8\% Y_2O_3$

The average value of tensile bond strength–adhesionof the coatings system with the thicknesses of bond coating/ceramic coating (0.1-0.11 mm/0.4-0.42 mm) was 38 MPa. Preheating of the surfaces provided for better distribution of particles along the substrate, thus increasing the bonding surface located between the molten particles and the substrate. The strong bond between the deposited particles and the coating is made possible since the molten particles shrink and anchor themselves to the rough surface. For a higher ratio of thicknesses (0.2-0.25 mm/0.25-0.28 mm), the strength was significantly higher - 64 MPa. Bond strength increases with the increase in bond coat thickness; this was expected because a thicker bond layer reduces the stress between the substrate and the ceramic layer. Figure 4 shows the microstructure of the coatings system with the following thicknesses of bond coating/ceramic coating: 0.1-0.11mm / 0.4-0.42mm and Figure 5 with the thicknesses: 0.2-0.25mm / 0.25-0.28 mm. In the micrographs, inter-boundaries between the substrate/bond coating and inter-boundaries of bond/ceramic coating are visible. Qualitative analysis showed that at the interface between the substrate and the deposited coatings there were no defects such as discontinuities of the layers, microcracks, macrocracks, delamination and flaking of the coating from the substrate, which is in accordance with the bond strength values. Analysis of the micrographs revealed that the average content of micropores in the bond coating was 1.7 %, while 15 % is the average contentwithin the layers of the ceramic coating. Figure 5 clearly shows the micropores in both of them, which are black and marked by arrows. In the Ni22Cr10Al1Y bond coating, oxide phases of a light greycolour are present in addition to the micropores.

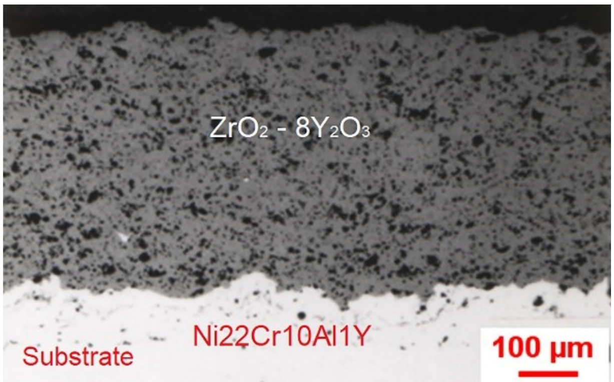

Figure 4. (OM) Microstructure of the $ZrO_2 8\% Y_2O_3$/ Ni22Cr10Al1Y coatings system

Slika 4. (OM) Mikrostruktura sistema prevlaka $ZrO_2 8\% Y_2O_3$/ Ni22Cr10Al1Y

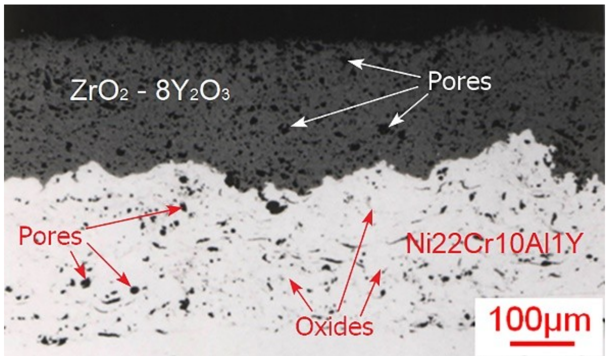

Figure 5. (OM) Microstructure of the $ZrO_2 8\% Y_2O_3$/ Ni22Cr10Al1Y coatings system, (bond/ceramic thickness ratio: 0.2-0.25 mm/0.25-0.28 mm)

Slika 5. (OM) Mikrostruktura sistema prevlaka $ZrO_2 8\% Y_2O_3$/ Ni22Cr10Al1 (vezna/keramička 0.2-0.25 mm/0.25-0.28 mm)

For clarity, Figure 6 shows the microstructure of the bond coating with a thickness of 0.2-0.25mm. The structure of the bond layers is lamellar. In the structure of the coating, two important Ni-based phases are present. The base of the coating is made of a solid solution of chromium and aluminium in nickel γ-Ni(Cr,Al) and intermetallic compounds of γ'-Ni_3Al dispersed in the base of the solid solution (light greycolour, marked with arrows). Through the layers of the bond coating at the inter-lamellar boundaries, dark grey oxide lamellae (NiO, Cr_2O_3 and α-Al_2O_3) are noticed; they are formed during the deposition of powder which reacts with oxygen from the air and the oxygen incorporated into the plasma jet from the surrounding atmosphere [32,33]. In terms of the microstructure, there are no unmolten particles. Neither microcracks nor macrocracks were observer through the cross-section of the ceramic layer.

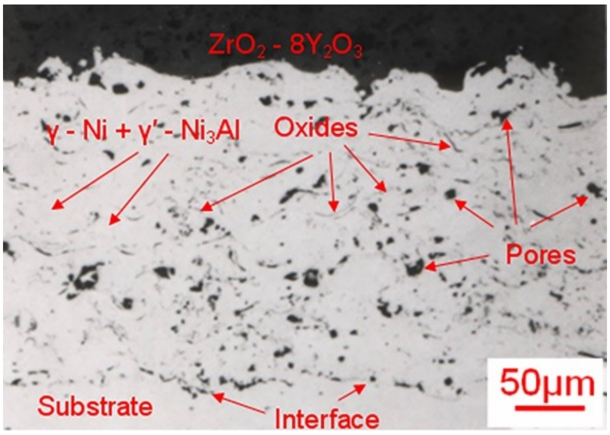

Figure 6. SEM image of the Ni22Cr10Al1Y bond coating

Slika 6. SEM slika vezne prevlake Ni22Cr10Al1Y

Figure 7 shows the SEM image of the surface morphology of the $ZrO_2$8%Y_2O_3 coating in the middle of the sample. Three overlapping splats are seen, indicating that the deposited particles were correctly and plastically well deformed on the previously deposited ceramic layer. The splats overlapping the edges are marked in Figure 7.

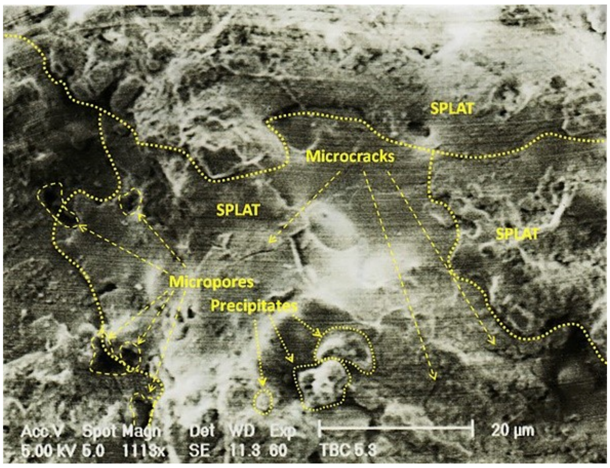

Figure 7. SEM Surface morphology of $ZrO_2$8%Y_2O_3 coatings in the middle of the sample.

Slika 7. SEM Morfologija površine $ZrO_2$8%Y_2O_3 u sredini uzorka

Ceramic powder particles, that have a high melting point, are fully molten in the core and upon the collision with the previously deposited layer, the molten ends of the particles were broken off and remained on the surface of the coating as precipitates. On the surface of the splats, precipitates up to 10 μm in size can be seen (marked with arrows). The microcracks present on the surface of the splats typically occur during the cooling of the deposited particles. Microcracks are a type of a problem which cannot be avoided. The reason behind the formation of microcracks lies in the stresses resulting from the thermal gradients in particles during the cooling phase and the difference in the thermal expansion coefficients of the deposited layers. The coating inner layers have a higher temperature relative to the coating surface and are exposed to tensile stresses. These stresses prevent the collection of particles onto the surface of the coating and are always greater than the tension of compacting of the particles which are cooling on the surface of the coating causing the formation of microcracks on the surface of the particles [33].

Figure 8 shows the SE image of the surface morphology of the ceramic coating at the sample edge-zone. One can observe an identical surface structure of the ceramic coating with a higher amount of precipitates. In the edge-zone, there were no large longitudinal cracks in the ceramics or separate segments of ceramics, which significantly affects the quality and functionality of the ceramic coating being used.

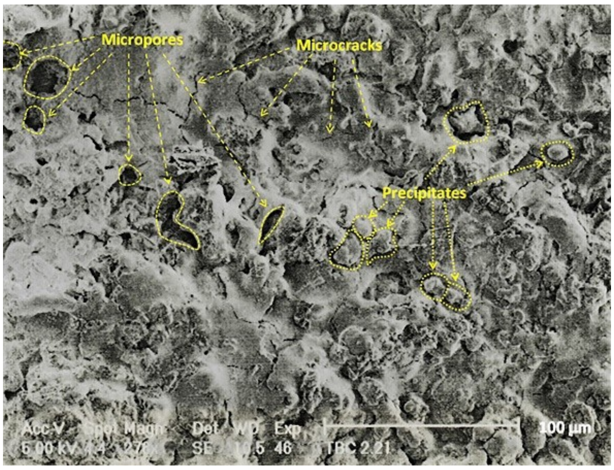

Figure 8. SEM Surface morphology of $ZrO_2$8%Y_2O_3 coatings at the edge of the sample

Slika 8. SEM Morfologija površine prevlake $ZrO_2$8%Y_2O_3 na ivici uzorka

In addition to the present microcracks and precipitates, micropores are visible on the surface of the ceramic coating. They are irregularly shaped and marked with arrows. The structure of the coating surface is good and typical for this type of ceramic.

4. CONCLUSIONS

For this paper, a system of $ZrO_2$8%Y_2O_3/ Ni22Cr10Al1Y coatings was produced using the APS process. We analysed the mechanical properties as well as the microstructure of coating layers in the deposited state and thermal insulation properties / thermal stability.

The coating system has good mechanical and structural properties. The microhardness values of the Ni22Cr10Al1Y bond coating were in the range from 386 to 414$HV_{0.3}$, and the $ZrO_2$8%Y_2O_3ceramic coating from 710 to 768$HV_{0.3}$. The layers were uniformly deposited across the entire cross-section. Within the layers of bond and ceramic coating, the content of micropores is 1.7 and 15%, respectively. The mean value of tensile bond strength depends on the ratio of the thickness of the bond coating/ceramic coating. For the higher ratio (0.2-0.25mm/0.25-0.28mm), average bond strength–adhesionwas significantly higher (64MPa) in comparison with 38MPa obtained for the lower ratio (0.1-0.11mm/0.4-0.42mm). Preheated substrates provided for better dispersions of particles and created more contact area between a coating and a substrate, which led to a higher value of adhesivebond strength.Tensile bond strength increases with the increase in bond thickness because the stresses between the substrate and top ceramic layer are reduced.

The microstructure of the coating consists of deformed and folded powder particles that form thin disks-splats in collision with the surface of the substrate.The base is made of a solid solution of chromium and aluminium in nickel γ-Ni(Cr,Al) and inter-metallic γ-Ni3Al compounds dispersed in the base of the solid solution. Between the lamellae of the solid solution, in the layers, NiO, Cr_2O_3 and α-Al_2O_3oxides are present; they are formed during the powder deposition. The $ZrO_2$8%Y_2O_3 ceramic coating is uniformly deposited on the bond layer, without unmolten particles, rough pores and cracks through the layers.

Acknowledgement

This work was supported by the Ministry of Education, Science and Technological Development of the Republic of Serbia ***(****Contracts No. 451-03-68/2021-14/200287,451-03-68/2020-14/200135****).***

5. REFERENCE

[1] K.A.Khor, L.Fu, V.J.P.Lim, P.Cheang (2000) The effects of ZrO2 on the phase compositions of plasma sprayed HA/YSZ composite coatings, Materials Sciiences, Eng.A, 276, 60–166.

[2] M.F.Morks, A.Kobayashi (2007) Microstructure and Mechanical Properties of HA/ZrO_2 Coatings by Gas Tunnel Plasma Spraying, Trans. JWRI, 36, 47–51.

[3] M.Mrdak, Č.Lačnjevac, M.Rakin (2018) Mechanical and structural features of Nb coating layers deposited on steel substrates in a vacuum chamber, Zastita materijala, 59(2), 167-172.

[4] M.Mrdak, Č.Lačnjevac, M.Rakin, N.Bajić (2018) Characterization of tantalum coatings deposited using vacuum plasma spray process, Zastita materijala, 59(4), 489-494.

[5] M.Mrdak, Č.Lačnjevac, M.Rakin, N.Bajić (2019) D.Veljić, Karakterizacija plazma sprej bioinertne prevlake $Al_2O_3$28tež.%MgO, Zastita materijala, 60(1), 44-49.

[6] P.Kumar, B.S.Dehiya, A.Sindhu (2018) Bioceramics for Hard Tissue Engineering Applications: A Review, International Journal of Applied Engineering Research, 13, 2744–2752.

[7] M.Dawlat, A. Moustafa (2018) Bioactive–hybrid–zirconia implant surface for enhancing osseointegration: an in vivo study, Int. J. Implant Dent.*,*4, 7-15.

[8] P.Christel, A.Meunier, M.Heller, J.P.Torre, C.N. Peille (1989) Mechanical properties and short-term in-vivo evaluation of yttrium-oxide-partially-stabilized zirconia, J. Biomed. Mater. Res., 23, 45–61.

[9] P.Fassina, N.Zaghini, A.Bukat, C.Piconi, F.Greco, S.Piantelli (1992) Yttria and calcia partially stabilized zirconia for biomedical applications. In Bioceramics and the Human Body; Ravagliogli, A.; Krajewski, A.; Elsevier Applied Science: London and New York, p. 223–229.

[10] R.C.Garvie, C.Urbani, D.R.Kennedy, J.C.McNeuer (1984) Biocompatibility of magnesia-partially stabilized zirconia (Mg-PSZ) ceramics, J. Mater. Sci., 19, 3224–3228.

[11] S.Deville, L.Gremillard, J.Chevalier, G.Fantozzi (2005) A Critical Comparison of Methods for the Determination of the Aging Sensitivity in Biomedical Grade Yttria-Stabilized Zirconia, J. Biomed. Mater. Res. Part B, 72, 239–245,

[12] S.Ban, H.Sato, Y.Suehiro, H.Nakahishi, M.Nawa, (2008) Biaxial flexure strength and low temperature degradation of Ce-TZP/Al_2O_3 nanocomposite and Y-TZP as dental restoratives, J. Biomed. Mater. Res. Part B, 87, 492–498.

[13] ISO 13356:2015 (2008) Implants for Surgery - Ceramic Materials Based on Yttria-Stabilized Tetragonal Zirconia (Y-TZP). International Organization for Standardization (ISO), 3rd ed.; Technical Committee: ISO/TC 150/SC 1 Materials.

[14] H.Lang, Th.Mertens (1990) The use of human osteoblast-like cells as an in vitro test system for dental materials, J. Oral Maxillofac. Surg., 48, 606–611.

[15] I.Dion, L.Bordenave, F.Lefebvre, R.Bareille, C. Baquey, J.R.Monties, P.Havlik (1994) Physico-chemistry and cytotoxicity of ceramics, J. Mater. Sci.: Mater. Medis., 5, 18–24.

[16] A.I.Kozelskaya, E.N.Bolbasov, A.S.Golovkin, A.I. Mishanin, A.N.Viknianshchuk, E.V.Shesterikov, A. Ashrafov, V.A.Novikov, A.Y.Fedotkin, I.A.Khlusov, S.I.Tverdokhlebov (2018) Modification of the Ceramic Implant Surfaces from Zirconia by the Magnetron Sputtering of Different Calcium Phosphate Targets: A Comparative Study, Materials, 11, 1949-1957.

[17] L.Nistor, M.Gradinaru, R.Rica, P.Marasescu, M. Stan, H.Manolea, A.Ionescu, I.Moraru (2019) Zirconia Use in Dentistry - Manufacturing and Properties, Curr Health Sci J, 45, 28–35.
[18] E.Marcelli, M.L.Costantino, T.Villa, P.Bagnoli, R.Zannoli, I.Corazza, L.Cercenelli (2014) Effect of intermediate ZrO_2-CaO coatings deposited by cold thermal spraying on the titanium-porcelain bond in dental restorations, The Journal of Prosthetic Dentistry, 112, 1201–1211.
[19] M.Saremi, A.Afrasiabi, A.Kobayashi (2007) Bond Coat Oxidation and Hot Corrosion Behavior of Plasma-Sprayed YSZ Coating on Ni Superalloy, Trans. JWRI, 36, 41–45.
[20] T.Sadowski, L.Marsavina (2011) Multiscale modelling of two-phase Ceramic Matrix Composites, Comp. Mater. Sci., 50, 1336–1346.
[21] S.Hertelé, N.Gubeljak, W.De Waele (2014), Advanced characterization of heterogeneous arc welds using micro tensile tests and a two-stage strain hardening (‘UGent’) model, Int. J. Press. Vessels Pip., 119, 87–94.
[22] D.Kozak, D.Damjanović, M.Katinić (2016) Integrity assessment of the butt weld joint with defect according to EN ISO 6520-1 series 400, Struct. Integr. Life, 16, 120–124.
[23] J.Djoković, R.Nikolić, D.Ilić, J.Vičan (2016) Dynamic crack growth along the elastic-plastic bimaterial interface, Struct. Integr. Life, 14, 161–165.
[24] B.Škorić, D.Kakaš, T.Gredić (1998) Influence of plasma nitriding on mechanical and tribological properties of steel with subsequent PVD surface treatments, Thin Solid Films, 317, 486–489.
[25] A.Dey, A.Sinha, K.Banerjee, A.K.Mukhopadhyay, (2014) Tribological studies of microplasma sprayed hydroxyapatite coating at low load, Mater. Technol., 29, B35–B40.
[26] Z.Azari, C.Casavola, C.Pappalettere, C.I.Pruncu (2012) Numerical simulation in coated materials: model of crack propagation in bi-material, Struct. Integr. Life, 12, 125–129.
[27] K.Khlifi, H.Dhiflaoui, L.Zoghlami, A.B.C.Larbi, (2015) Study of mechanical behavior, deformation, and fracture of nano-multilayer coatings during microindentation and scratch test, J. Coat. Technol. Res., 12, 513–524.
[28] Material Product Data Sheet (2012) AMDRY 9624, Nickel chromium aluminum yttrium (NiCrAlY) thermal spray powders, 2012, DSMTS-0102.0, SulzerMetco.
[29] Material Product Data Sheet (2012) Metco 204NS, 8% Yttria Stabilized Zirconia Agglomerated and HOSP™ thermal spray powders, DSMTS-0001.2, SulzerMetco.
[30] Turbojet Engine – Standard Practices Manual (PN 582005) (2002) Publisher: Pratt & Whitney Aircraft Group, East Hartford.
[31] O.V.Penkov, M.Khadem, W.S.Lim, D.E.Kim (2015) A review of recent applications of atmospheric pressure plasmajets for materials processing, J. Coat. Technol. Res., 12, 225–235.
[32] ASM Handbook (1992) Alloy Phase Diagrams; Editor: Baker, H.; Publisher: ASM International, Ohio, USA; Volume 3.
[33] M.Mrdak (2012) Study of the properties of plasma deposited layers of nickel-chrome-aluminum-yttrium coatings resistant to oxidation and hot corrosion, Military Technical Courier, 60, 182–201.

IZVOD

KARAKTERIZACIJA BIOKOMPATIBILNIH SLOJEVA $ZrO_2 8\% Y_2O_3$ KOJI SE KORISTE U KOMBINACIJI SA DRUGOM KERAMIKOM ZA MODIFIKACIJU POVRŠINE IMPLANTATA

Cilj ovog rada bio je da se deponuju višenamenski slojevi prevlake $ZrO_2 8\% Y_2O_3$ primenom plazma sprej tehnologije, a zatim da se karakterišu takvi slojevi. U kombinaciji sa drugom biomedicinskom keramikom, ova prevlaka je namenjena primeni u modifikaciji površine implantata. Ispitivanje je bilo usredsređeno na mehanička svojstva i mikrostrukturu slojeva. Korišćenjem atmosferskog plazma spreja, dupleks sistem prevlaka $ZrO_2 8\% Y_2O_3$ / Ni22Cr10Al1Y nanet je na nerđajući čelik X15Cr13, sa dve različite debljine vezne i keramičke prevlake. Mikrostruktura je analizirana pomoću optičkog mikroskopa, uključujući procenu sadržaja mikro pora. Morfologija čestica praha i površina keramičkih prevlaka ispitivane su na skening elektronskom mikroskopu (SEM). Kvalitet slojeva $ZrO_2 8\% Y_2O_3$ čini ih pogodnim za nanošenje i kombinaciju sa drugim materijalima kako bi se stvorio sistem biomedicinskih ili multifunkcionalnih prevlaka.

***Ključne reči**: atmosferski plazma sprej, $ZrO_2 8\% Y_2O_3$, Ni22Cr10Al1l, mikrostruktura, među-površina, mikrotvrdoća, čvrstoća spoja.*

Naučni rad
Rad primljen: 28. 06. 2021.
Rad prihvaćen: 24. 07. 2021.
Rad je dostupan na sajtu: www.idk.org.rs/casopis